IMPEDANCE CHARACTERIZATION OF TRANSPARENT AND FLEXIBLE CARBON NANOTUBES THIN FILM NETWORKS

M. Z. Iqbal[1,2*], Jonghwa Eom[2], J. Pérez-Puigdemont[1], N. Ferrer-Anglada[1*]
[1]Applied Physics Department, Universitat Politècnica de Catalunya (UPC), Campus Nord B4, J. Girona 3-5, 08034 Barcelona, Spain
[2]Department of Physics and Graphene Research Institute, Sejong University, Seoul 143-747, Korea
* Corresponding author (nuria@fa.upc.edu , zahir@fa.upc.edu)

1 Introduction

Single-walled carbon nanotubes (SWCNTs) have attracted significant interest in many fields due to their remarkable electrical, optical, mechanical and thermal properties. In particular, the excellent properties of SWCNTs make them suitable for application in transparent and flexible electrodes [1-5]. Our objective was to study and characterize the SWCNTs composites, a necessary step for their applications. Thus, when SWCNTs are deposited on an insulating, transparent substrate, conductive and transparent films (T=80%-90%) in the visible-NIR range are achieved [6 - 9]. These thin films may be used as transparent electrodes in organic electronic devices because they have greater mechanical flexibility than indium tin oxide. They are particularly well suited as electrodes in organic solar cells as they increase their performance [10]. In many cases, flexibility is the most important parameter, i.e. in solar cells, for achieving good integration in the building architectural structure. The study of electrical and optical properties of SWCNTs thin films are useful for transparent and flexible network applications in different kind of devices including sensors, transistors and transparent electrodes.

2 Experimental

The first step in building electrodes is to obtain a transparent conductive network of nanotubes over a desired substrate, polypropylene carbonate (PPC). An electrode was prepared of single-walled CNTs as described previously [2]. Two-probe impedance measurements were performed using an Agilent 4294A precision impedance analyser in the range 40 Hz to 110 MHz on rectangular samples and a co-axial (Corbino geometry) sample when using an Agilent E8362B impedance analyser in the frequency range 10 MHz to 20 GHz. The relative densities of thin films were estimated by optical absorption spectroscopy. Raman spectroscopy is used to assess the purity of SWCNTs network. Atomic force microscopy studies were performed to see the morphology and homogeneity of SWCNT network on PPC substrate.

3 Characterization

3.1 Impedance analysis

The analysis of the absolute impedance value in the frequency range observed gave us two major parameters: the low frequency impedance or DC resistance (R_{DC}) and the cut-off frequency (ω_0). These two values depend on the density of the SWCNTs thin film, generally as the density increases, the DC resistance decreases, while the cut-off frequency increases with the density of the SWCNTs [11]. Here, we used eight batches of samples with different SWCNTs densities. These eight batches further divided in four different categories, all samples having the same width (W= 0.5cm) but different lengths. Three of them (L= 1.5cm, 3cm and 6cm) were characterized by two probe method and one of them (L= 0.5cm) was characterized by a co-axial method. A schematic diagram of co-axial method is shown in figure 1. Figure 2 shows the log-log dependence of impedance on frequency of rectangular shape samples. The impedance of the thin film starts to decrease at a constant rate at a particular frequency, defined as the cut-off frequency. This phenomenon is due to the fact that during a half period of the electric field, $T/2 < \pi / \omega_0$, the electrons do not have enough time to cross all the junctions on their way through the nanotubes random network from one contact pad to another. As the frequency increases, the electrons cross fewer junctions, which act as potential barriers. As a result of this, the electrons

dissipate less energy in the random network and the impedance decreases. The cut-off frequency ω_0 at which the impedance starts to decrease is related to the mean distance between the junctions in the random nanotubes network. The high frequency Corbino geometry impedance $Z_s(\omega)$ was measured by [12]

$$Z_s(\omega) = Z_0 \frac{2\pi}{\ln(b/a)} \frac{1+\hat{S}_{11}(\omega)}{1-\hat{S}_{11}(\omega)} \qquad (1)$$

Where Z_0= 50Ω is the characteristic impedance of the co-axial transmission line and a=1.9 mm and b=0.5 mm are the inner and outer diameters of the sample contact, respectively, $\hat{S}_{11}(\omega)$ is the scattering parameter. Figure 4 shows the impedance dependence Re(Z) at ω_0, on cut-off frequency ω_0 for different samples. The red line represents those values for samples with length L=1.5cm measured by two probe method (upper black points on red line) and L=0.5cm measured by co-axial method (lower black points on red line). Blue and green lines represent these values for samples with lengths L=3cm and L=6cm, respectively, measured by two probe method. We observed that different sample geometry gives different ω_0, but all of them lie on same line and slop. We also observed that the value of impedance measured by co-axial method is quite lower than two probe method. This is mostly due to the different geometry and size of samples, and also due to the different contact resistance: we used silver paste contacts in the two probe samples, while in co-axial method the tip of SMA connector directly touches to the surface of film, this reduces the contact resistance and results a lower impedance measured.

3.2 Optical absorption analysis

Figure 5 shows the optical transmittance versus wavelength for various SWCNTs network films on PPC substrate. Highly dense SWCNTs network shows low transmittance whereas light dense shows hight transmittance. The inset shows the optical transmittance as a function of sheet square resistance. The less density of SWCNT corresponds to the maximum transparency (T close to 95%). As all the SWCNT samples were obtained using the same method and come from the same batch, we use % transmittance as an estimation of SWCNTs density. These measurements were helpful in order to optimize the conditions for obtaining thin films both electrically conductive and transparent, and by varying the density of SWCNT networks we can tune these properties for different applications.

3.3 Raman spectroscopy

The most characteristic features in Raman spectra of SWCNTs are reported in Ref. [13]. The inter band with defect-induced vibration (D-mode) lies between 1200 and 1400 cm^{-1}, and the high energy range 1500-1800 cm^{-1}, belongs to the tangential mode (G and G´ mode). All these modes are shown in figure 6. The film is constituted by scattered aggregates of nanotubes clusters and the surface state is very irregular. In the most concentrated sample, a random distribution of nanotubes is observed. The ratio between the D band and G band is a good indicator of the quality of the samples. If these both bands have similar intensity this indicates a high quantity of structural defects. Therefore, the G/D ratio allows us to assess the purity of SWCNTs network. In our samples the G/D ratio is more than 2 which indicates a high purity SWCNTs network.

3.4 Atomic force microscopy

To verify the uniform dispersion of SWCNT on PPC substrate and to check the RMS roughness atomic force microscopy studies were performed. Figure 7 corresponds to AFM image from sample-7 (a quite light sample), it shows a large area of SWCNT network on PPC substrate. As observed from topography map on figure 7, the cluster network is distributed on the whole substrate. The RMS roughness calculated is around 12 nm. The inset shows the line profile taken by drawing the line in the middle of topography image which gave the average thickness of the SWCNT film 25 nm.

4 Conclusions

We prepared SWCNTs networks on transparent flexible substrates with different densities by spray. The electrical impedance Z was measured at different frequencies, in the range from 40 Hz to 110 MHz and 10MHz to 20 GHz.

The observed values of impedance with the same SWCNT density and different sample geometry gives the same impedance values, but different cut-

off frequency ω_0. Nevertheless, all of them lie on a line showing rather the same slop, on a log-log representation of the real part of impedance Re (Z) versus the cut-off frequency ω_0, for SWCNT thin film networks with different densities and geometries. The impedance Z at low frequency, similar to R_{DC}, decreases when increasing SWCNTs density, estimated by optical transmittance, as expected. The ω_0 is displaced to higher values when increasing the SWCNTs density and varies with sample geometry and size, but the correlation between Z and ω_0 is the same. Raman spectra shows a G/D lines ratio that is more than 2, which indicates a high purity of SWCNTs network.

The topographical atomic force microscopy image shows that the SWCNT network is distributed on the whole substrate, the SWNTs thin film is constituted by aggregates of nanotubes clusters and the surface state is very irregular. In the most concentrated sample, a random distribution of nanotubes is observed. For a light simple, the RMS roughness calculated is around 12 nm and the average thickness of film is of the order of 25 nm.

As significative values, the sheet resistance is as low as 2.51±0.05 kΩ/sq for T=65% and 7.97±0.05 kΩ/sq for T=85%.

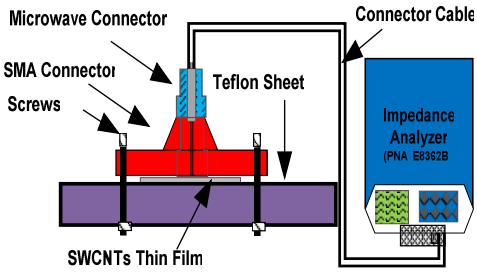

Fig. 1. The schematic diagram of co-axial method.

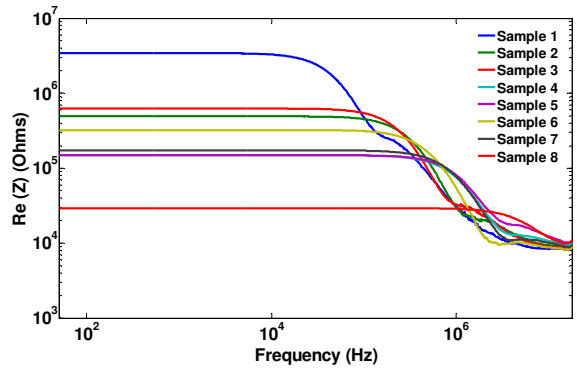

Fig. 2. The frequency dependence of the square impedance modulus.

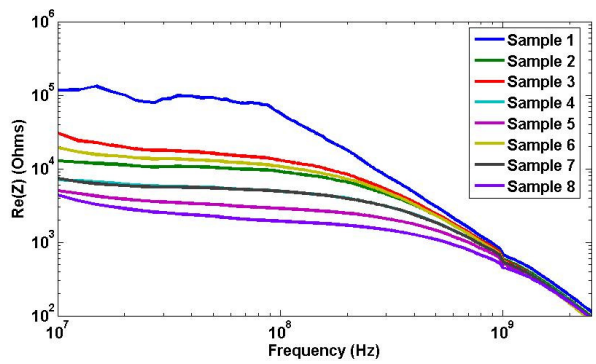

Fig. 3. Impedance versus frequency of SWCNT thin film networks by coaxial (panel mount SMA connector with inner and outer diameters a=0.5 mm and b=1.9 mm respectively) method.

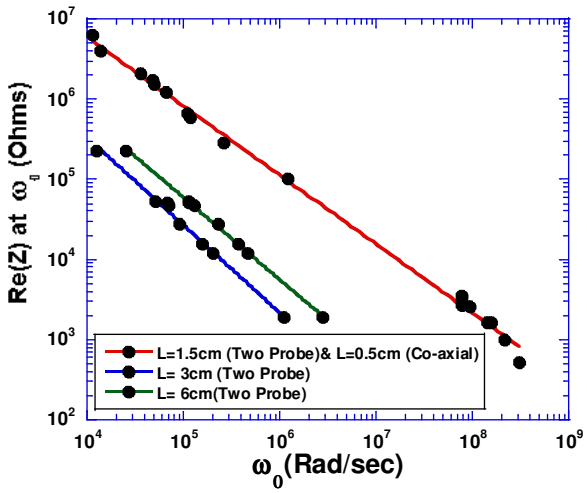

Fig. 4. The real part of impedance Re(Z) versus the cut-off frequency ω_0 of SWCNT thin film networks with different densities and geometries by two probe L=1.5cm, L=3cm, L=6cm, and coaxial contacts (Corbino geometry with inner and outer diameters a=1.9 mm and b=0.5 mm respectively) L=0.5cm.

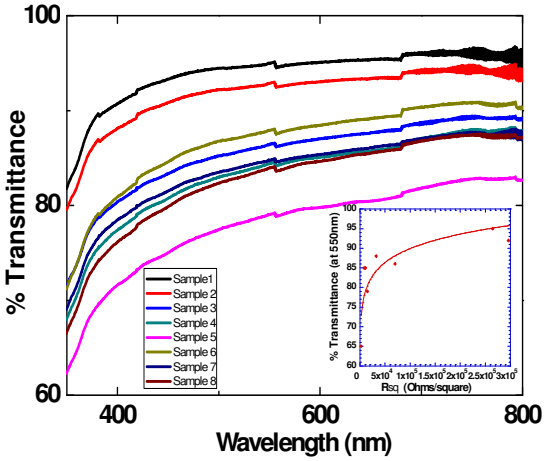

Fig. 5. Transmittance versus wavelength for various SWCNTs-network films on PPC substrate. Inset: Shows the optical transmittance %T (at 550nm) versus sheet resistance, Rsq.

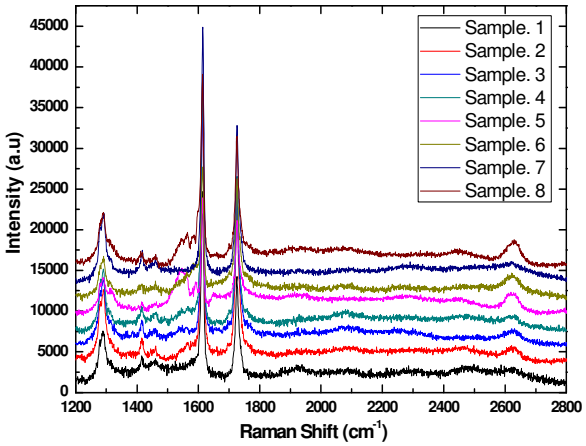

Fig. 6. Raman spectra of SWCNTs thin film network on PPC substrate with different densities.

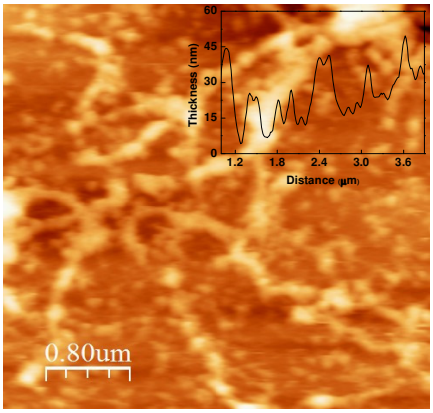

Fig. 7. AFM image of a thick nanotube thin film area 4x4 $(\mu m)^2$. The inset shows the line profile taken by drawing the line in the middle of topography image which gave the average thickness of the SWCNT film 25 nm and RMS around 12 nm.

5 Acknowledgement

This work was supported by Basic Science Research Program (2011-0002861) and Priority Research Centers Program (2010-0020207) through the National Research Foundation of Korea (NRF) funded by the Ministry of Education, Science and Technology.

6 References

[1] S. Bae, H. Kim, Y. Lee, X. Xu, J. Park, Y. Zheng, J. Balakrishnan, T. Lei, H. R. Kim, Y. I. Song, Y. Kim, K. S. Kim, B. Özyilmaz, J. Ahn, B. Hee Hong and S. Iijima, *"Roll-to-roll production of 30-inch graphene filmsfor transparent electrodes",* Nanotechnology 5, pp 574–578, 2010.

[2] N. Ferrer-Anglada, M. Kaempgen, U. Dettlaff-Weglikovska, V. Skákálova and S. Roth, "*Transparentand carbon nanotube/polypyrrole and carbon nanotube/polyaniline pH sensors¨* Phys. Stat. Sol. (b) 13, 3519, 2006.

[3] N. Ferrer-Anglada, J. Pérez-Puigdemont and S. Roth, *¨Impedance and quantitative TGA characterization of transparent carbon nanotube thin films¨* phys. stat. sol. (b) 245, No. 10, pp 2276-2279, 2008.

[4] A. Southard, V. Sangwan, J.Cheng, E. D. Williams, M. S. Fuhrer, *¨Solution-processed single walled carbon nanotube electrodes for organic thin-film transistors",*Organic Electronics, 2009 doi: 0.1016/j.orgel.2009.09.001

[5] O. Hjortstam, P. Isberg, S. Soderholm, and H. Dai, *"Can we achieve ultra-low resistivity in carbon nanotube-based metal composites?"* Appl. Phys. A 8, pp 1175-1179 (2004).

[6] N. Ferrer-Anglada, M. Kaempgen, S. Roth et al., "*Synthesis and characterisation of carbon nanotube-conducting polymer thin films",* Diamond Relat. Mater. 13, 156 (2004).

[7] Z. Wu, Z. Chen, X. Du, J. Logan et al., *Transparent, Conductive Carbon Nanotube Films,* Science 305, 1273 (2004).

[8] B. Parekh, G. Fanchini, G. Eda, and M. Chhowalla, "*Improved conductivity of transparent single-wall carbon nanotube thin films via stable post-deposition functionalization",* Appl. Phys. Lett. 90, 121193 (2007).

[9] E. Artukovic, M. Kaempgen, D.S. Hecht, S. Roth, G. Grüner, *¨Transparent and flexible carbon nanotube transistors ¨*Nano Letters 5, pp 757-760, 2005.

[10] L. Hu, G. Grüner, M.W. Rowell, M.A. Topinka, M.D. McGehee, H. Prall, G. Dennler, N.S. Sariciftci, *"Organinc Solar Cells with Carbon Nanotube Network Electrodes",* Applied Physics Letters, 88, 233506 (2006).

[11] H. Xu, S. Zhang, S. M. Anlage, L. Hu, G. Grüner, "*Frequency- and electric-field-dependent conductivity of single-walled carbon nanotube networks of varying density",* Phys. Rev. B 77, 075418, 2008.

[12] H. Xu, S. M. Anlage, L. Hu, and G. Gruner, *¨Microwave shielding of transparent and conducting single-walled carbon nanotube films¨* Appl. Phys. Lett. 90, 183119, 2007.

[13]. S. Reich, C. Thomsen, and J. Maultzsch, in: "*Carbon Nanotubes: Basic Concepts and Physical Properties"* (Wiley-VCH, Berlin, 2004), p. 135.